

# Mathematical Modeling of Voltage-Lift Technique for Multiphase DC–DC Converter

Suchita Singh <sup>1</sup>, Varsha Mehar <sup>2</sup><sup>1,2</sup>Department of Electrical Engineering, RKDF University, Bhopal, India

\* Corresponding Author: Suchita Singh

Manuscript Received:

Manuscript Accepted:

**Abstract:** *Now a day's, power converters are very critical in low powered electronic devices like cell phone, tablet, laptop computers and other handheld devices, due to its smaller size, light weight, high efficiency and high power density. In this paper, a novel voltage lift technique based multiphase DC–DC converter is proposed. There are many applications required for transformer, coupled inductances and sequential connections in the proposed multiphase converter topology. In this paper, the process of proposed multiphase DC–DC converter in continuous conduction mode (CCM) and discontinuous conduction mode (DCM) are discussed, and mathematical equations of current and voltage for the inductors and capacitors are derived with details. So, the result of critical inductance and the operating of the proposed DC–DC converter between CCM and DCM are presented. Using simulation results, the performance of the proposed converter based on presented technological issues is verified.*

**Keywords:** *DC–DC Converter, Multiphase, Voltage-Lift, Continuous Conduction Mode (CCM), Discontinuous Conduction Mode (DCM).*

## I Introduction

Power converters are required to convert one form of electric energy to another. This paper introduces fundamental concepts of DC–DC conversions and applications. It can barely imagine the lifestyle without the conversion and processing activities which use electrical energy, and its supply.

Power supply technology is an enabling technology that allows us to build and operate electronic circuits and systems. All active electronic circuits, both digital and analog, require power supplies. Many electronic systems require several DC supply voltages [1, 2]. Power supplies are widely used in computers, telecommunications, instrumentation equipment, aerospace, medical, and defense electronics. A DC supply voltage is usually derived from a battery or an ac utility line using a transformer, rectifier, and a filter. The resultant raw dc voltage is not constant enough and contains a high ac ripple that is not appropriate for most applications. Voltage regulators are used to make the dc voltage more constant and to attenuate the ac ripple [3, 4].

A power supply is a constant voltage source with a maximum current capability. There are two general classes of power supplies: regulated and unregulated. The output voltage of a regulated power supply is automatically maintained within a narrow range, e.g., 1 or 2% of the desired nominal value, in spite of line voltage, load current, and temperature variations. Regulated dc power supplies are called dc voltage regulators. There are also DC current regulators, such as battery chargers.

Figure 1 shows a classification of regulated power supply technologies. Two of the most popular categories of voltage regulators are linear regulators and switching-mode power supplies (SMPS). There are two basic linear regulator topologies: the series voltage regulator and the shunt voltage regulator. The switching-mode voltage regulators are divided into three categories: pulse-width modulated (PWM) DC–DC converters, resonant DC–DC converters, and switched-capacitor (also called charge-pump) voltage regulators. In linear voltage regulators, transistors are operated in the active region as dependent current sources with relatively high voltage drops at high currents, dissipating a large amount of power and resulting in low efficiency. Linear regulators are heavy and large, but they exhibit low noise level and are suitable for audio applications [5].

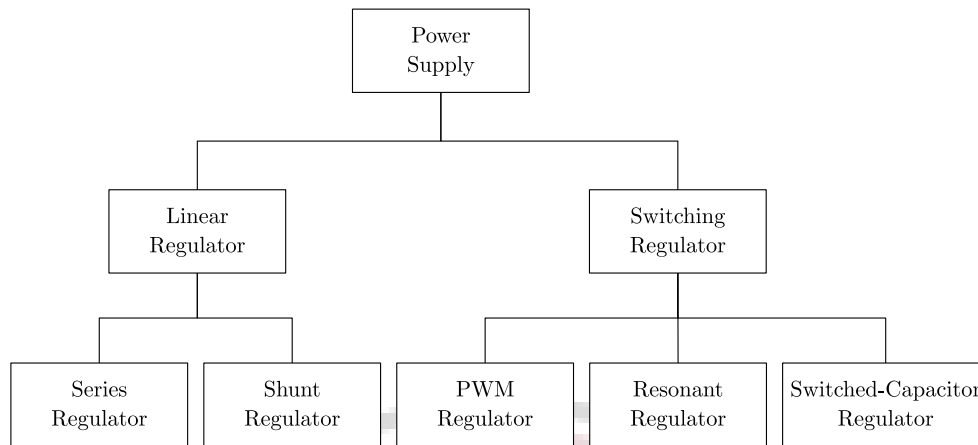


Figure 1: Categories of Power Supply technology

### I-A Switching-Mode Converter and Regulator

In switching-mode converters, transistors are operated as switches, which inherently dissipate much less power than transistors operated as dependent current sources [6, 7]. The voltage drop across the transistors is very low when they conduct high current and the transistors conduct a nearly zero current when the voltage drop across them is high. Therefore, the conduction losses are low and the efficiency of switching-mode converters is high, usually above 80% or 90%. However, switching losses reduce the efficiency at high frequencies. Switching losses increase proportionally to switching frequency. Linear and switched-capacitor regulator circuits (except for large capacitors) can be fully integrated and are used in low-power and low-voltage applications, usually below several watts and 50 V. PWM and resonant regulators are used at high power and voltage levels. They are small in size, light in weight, and have high conversion efficiency [8, 9].

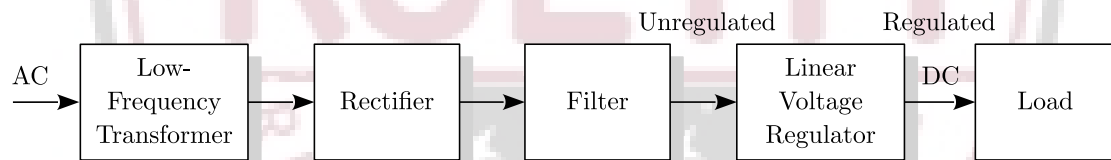


Figure 2: AC-DC Power Supply with a Linear Regulator

Figure 2 shows block diagrams of two typical AC-DC power supplies that convert the widely available AC power to DC power. The power supply contains a DC linear voltage regulator, whereas the power supply of Figure 3 contains a switching-mode voltage regulator. The power supply shown in Figure 2 consists of a low-frequency step-down power line transformer, a front-end rectifier, a low-pass filter, a linear voltage regulator, and a load. The nominal voltage of the ac utility power line is 110 V rms in the United States and 230 V rms in Europe. However, the actual line voltage varies

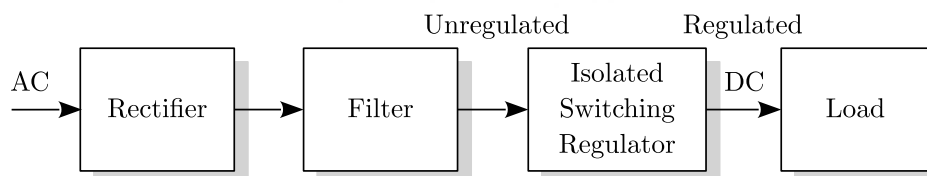


Figure 3: AC-DC Power Supply with a Switching-Mode Voltage Regulator

within a range of about  $\pm 20\%$  of the nominal voltage. The frequency of the AC line voltage is very low (50 Hz in India and Europe, 60 Hz in United States, 400 Hz in aircraft applications, and 20 kHz in space applications). The line transformer provides dc isolation from the ac power line and reduces a relatively high line voltage to a lower voltage (ranging usually from 5 to 28 V rms). Since the frequency of the AC line voltage is very low, the line transformer is heavy and bulky. The

output voltage of the front-end rectifier/filter is unregulated and it varies because the peak voltage of the ac line varies. Therefore, a voltage regulator is required between the rectifier/filter and the load. There still exists a need for universal power supplies that can accept any utility line voltage in the world, ranging from 85 to 264 V rms.

The power supply shown in Figure 3 consists of a front-end rectifier, a low-pass filter, an isolated DC–DC switching-mode voltage regulator, and a load. It is run directly from the ac line. The AC voltage is rectified directly from the ac power line, which does not require a bulky low-frequency line transformer. Hence, such a circuit is called an off-line power supply (plug into the wall). The switching-mode voltage regulator contains a high-frequency transformer to obtain dc isolation for the entire power supply. Since the switching frequency is much higher than that of the ac line frequency, the size and weight of a high-frequency transformer as well as inductors and capacitors is reduced. The switching frequency usually ranges from 25 to 500 kHz. To avoid audio noise, the switching frequency should be above 20 kHz. A PWM switching-mode voltage regulator generates a high-frequency rectangular voltage wave, which is rectified and filtered. The duty cycle (or the pulse width) of the rectangular wave is varied to control the DC output voltage. Therefore, these voltage regulators are called PWM DC–DC converters [10–12].

## II Related Work

The Full Bridge high-power-factor converter presented by Mario Ponce-Silva *et al.* [13] has the inherent capability to become attractive power supplies for telecommunications energy systems. The full-bridge type circuit configuration can be selected for the large-capacity power supplies. While power supplies for telecommunications energy systems normally require the isolation between the input and the output sides, if one uses the circuit configurations in the input and output isolation can be realized with a high frequency transformer link.

Gerry Moschopoulos *et al.* [14] presented “Single-phase single-stage power-factor-corrected converter topologies”, these are related to AC-DC and AC-AC converters that are classified on the basis of the frequency of the input ac source, the presence of a dc-link capacitor, and the type of control used (resonant or pulse width modulation). Considering practical design constraints, it is possible to effectively employ many single-stage converter topologies in a wide range of applications.

Tomokazu Mishima *et al.* [15] presented a novel high frequency transformer linked full-bridge type soft-switching phase-shift pulse width modulation (PWM) control scheme DC-DC power converter is presented. A tapped inductor filter is implemented in the proposed soft-switching converter topology to achieve wide load variation range soft-switching pulse width modulation (PWM) constant frequency operation of the DC-DC converter, to minimize circulating current.

Pubali Mitra *et al.* [16] presented research with ordinary PI controllers the dynamic response of the buck converter output voltage caused by load change exhibits large dynamic deviations from the desired steady state output value, with state space controller the dynamic response of the buck converter exhibits fast load response with small dynamic deviations from the desired steady state output value. It exhibits steady state error. Therefore, an approach with outer PI controller in addition to the internal state space controller and disturbance observer.

## III Proposed Method

Voltage-lift modeling is one of the most important techniques in designing the multiphase DC–DC converters. In this technique, by using the natural features of the energy storable elements (capacitor and inductance), the output voltage gain is increased step by step, and also by using the simple topology, the circuit characteristics is improved. Figure 4 shows the proposed boost dc–dc converter. As shown in Figure 4, the proposed converter consists of inductances  $L_2$  and  $L_3$ , capacitors  $C_1$  and  $C_2$  and diodes  $D_2$ ,  $D_3$  and  $D_4$  in addition to the conventional DC–DC converter to increase transmission voltage gain. In other word, the required elements for voltage-lift modeling technique include of these additional elements. However, the proposed structure has some drawbacks. The proposed structure uses two switches and four diodes, most of them experiencing a hard switching. In next sections, the voltage and current of each element in continuous conduction mode (CCM) and discontinuous conduction mode (DCM) are calculated.

### III-A Analysis of Proposed Multiphase Converter in Continuous Conduction Mode (CCM)

In the time interval of  $T_{on}$  that the switch  $S_1$  is turned on and the switch  $S_2$  is turned off, the inductance current of  $L_1$  is linearly increased and as a result its storage energy is increased. In this time interval, the diodes of  $D_1$ ,  $D_3$  and  $D_4$  are connected reversely, and the diode of  $D_2$  is directly connected. In this condition, the load is connected in series with inductances  $L_2$  and  $L_3$ , and capacitors  $C_1$  and  $C_2$ . In this condition, the currents of the load and capacitor  $C_3$  are provided by the inductances  $L_2$  and  $L_3$ , and by discharging the capacitors  $C_1$  and  $C_2$ . Therefore, the voltage of capacitors  $C_1$  and  $C_2$  are reduced. By reducing the current of inductances  $L_2$  and  $L_3$ , the supplied energy in them are decreased.

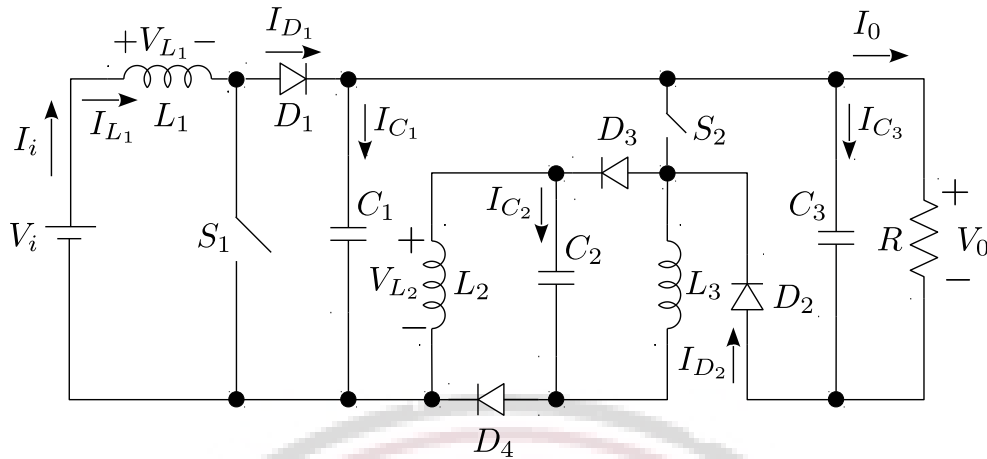


Figure 4: Structure of Proposed Multiphase DC-DC Converter

In the time interval of  $T_{off}$  that the switch  $S_1$  is turned off and the switch  $S_2$  is turned on, the diodes of  $D_1$ ,  $D_3$  and  $D_4$  are directly connected and the diode of  $D_2$  is reversely connected. In this time interval, because of charging the capacitors  $C_1$  and  $C_2$ , the inductance current of  $L_1$  is reduced and so its storage energy is decreased. By increasing the storage energy of capacitors  $C_1$  and  $C_2$ , their voltage is also increased. In addition, the current of the inductances  $L_2$  and  $L_3$  are increased because of increasing their storage energies. In this time interval, the load current is provided by discharging the capacitor  $C_3$ .

The voltage and current waveforms of the converter's elements in a duty cycle by considering in continuous conduction mode (CCM).

$$T = T_{on} + T_{off} \tag{1}$$

Following, by assuming the high capacitance value for  $C_1$ ,  $C_2$  and  $C_3$ , the equations of the current and voltage of each circuit's element are calculated in steady state and for two time intervals of  $T_{on}$  and  $T_{off}$ .

### III-A.1 Current and Voltage Equations of the Inductance $L_1$

In this sub-section, the main aim is calculation the voltage and current equations of the inductance of  $L_1$  in a duty cycle. In the time interval of  $T_{on}$  that the switch  $S_1$  is turned on and the switch  $S_2$  is turned off, the inductance of  $L_1$  is directly connected to the voltage source of  $V_i$ . In this condition, the current value of the inductance  $L_1$  is linearly increased from its minimum magnitude ( $I_{LV1}$ ) to maximum value ( $I_{LP1}$ ), so, its storage energy is increased. In the time interval of  $T_{off}$  that the switch  $S_1$  is turned off and the switch  $S_2$  is turned on, the inductance of  $L_1$  is series connected to the combination of parallel connection of the inductances  $L_2, L_3$  and capacitors  $C_1$  and  $C_2$ . Because of discharging the capacitors  $C_1$  and  $C_2$ , the current value of the inductance  $L_1$  is reduced from it maximum value to its minimum one and its storage energy is decreased. By applying KVL to the indicated circuit and considering the equation between voltage and current inductance, the equation voltage of the inductance  $L_1(v_{L1,1})$  in the time interval of  $T_{on}$  is obtained as follows:

$$V_i = L_1 \frac{di_{L1,1}}{dt} \tag{2}$$

$$= L_1 \frac{\Delta i_{L1}}{T_{on}} \tag{3}$$

The above equation can be rewritten as follows:

$$i_{L1,1} = \frac{V_i}{L_1}t + I_{LV1} \tag{4}$$

At the end of this operating mode, the above equation could be rewritten as follows:

$$i_{L1,1}|_{t=T_{on}} = I_{LP1} \tag{5}$$

In the time interval of  $T_{\text{off}}$ , by applying KVL and considering the equation between voltage and current inductance, the voltage of the inductance  $L_1(v_{L_{1,2}})$  in the time interval of  $T_{\text{off}}$  is calculated as follows:

$$V_i - v_{C_{1,2}} = L_1 \frac{di_{L_{1,2}}}{dt} \quad (6)$$

$$= -L_1 \frac{\Delta i_{L_1}}{T_{\text{off}}} \quad (7)$$

From Equation 7, it is obtained that:

$$i_{L_{1,2}} = -\frac{V_i - v_{C_{1,2}}}{L_1} t + I_{LP_1} \quad (8)$$

At the end of this operating mode, we have:

$$i_{L_{1,2}}|_{t=T_{\text{off}}} = I_{LV_1} \quad (9)$$

### III-A.2 Current and Voltage Equations of Capacitors $C_1$ and $C_2$

In the time interval of  $T_{\text{on}}$ , the capacitor of  $C_1$  is discharged and so its storage energy is decreased. By reducing its storage energy, its voltage is decreased from its maximum value ( $V_{CP_1}$ ) to the minimum value ( $V_{CV_1}$ ). In the time interval of  $T_{\text{off}}$ , the capacitor of  $C_1$  is charged by using the current of the inductance  $L_1$ , and as a result, its voltage is increased from maximum value to the minimum one that leads to increase the storage energy in it. By using the relation of the inductance voltage balancing rule in steady state for the inductance of  $L_1$  and considering the equation between voltage and current inductance and Equation 7 into it, and by determining  $T_{\text{off}}$  as a new time offset, we have:

$$\int_0^{T_{\text{on}}} V_i dt + \int_0^{T_{\text{off}}} (V_i - v_{C_{1,2}}) dt = 0 \quad (10)$$

By defining duty cycle ( $D$ ), the average voltage value of the capacitor  $C_1$  is calculated as follows:

$$v_{C_{1,2}} = \frac{1}{1-D} V_i \quad (11)$$

By considering the high enough value of the capacitor  $C_2$ , its average voltage value ( $v_{C_2}$ ) is obtained as follows:

$$v_{C_1} = v_{C_2} \quad (12)$$

In addition, the below equation is resulted as:

$$i_{C_{1,1}} = -i_{C_{2,1}} = -i_{L_{2,1}} = -i_{L_{3,1}} \quad (13)$$

## IV Result

The simulation results are provided to demonstrate mathematical modeling of voltage-lift operation of the proposed converter in continuous conduction mode (CCM). The specification of the implemented circuit is presented in Table 1. Figure 5 represents the simulation results of presented converter in continuous conduction mode (CCM). Figure 5(a)–(c) illustrate the voltage waveforms of inductances, diodes and load, respectively. As it can be seen in Figure 5, the output voltage is reached to 96 V by considering the presented values in Table 1. As it mentioned, all simulation results agree well with the theoretical analysis and simulation results.

Meanwhile, the efficiency ( $\eta$ ) obtained operating with nominal load is equal to 90% by considering the presented values in Table 1. The comparison of theoretical and simulation voltage gain is done by various duty ratio.

As it can be seen, the voltage gain of proposed converter is decreased because of the non-ideal elements, but the high voltage is achieved. The comparison of proposed converter efficiency for full load and light load is shown in Figure 6. The resistances of full load and light load were considered  $R = 500 \Omega$  and  $R = 10 \Omega$ , respectively. As it can be seen in Figure 6, the efficiency measured for full load is higher than light load for all  $D$ . The efficiency measured was reached to 96.5% with considering Table 1.

In addition, the comparison of the experimental converter efficiency changes with the load and input voltage variations can be discussed by Figure 7. These comparison was done by considering Table 1 at  $D = 0.5$ . As it can be seen in Figure 7,

Table 1: Parasitic Parameters of Converter for Laboratory Prototype

Parameters	Value
$r_{L1}$	15 m $\Omega$
$r_{L2} = r_{L3}$	20 m $\Omega$
$r_{C1} = r_{C3}$	15 m $\Omega$
$r_{C3}$	10 m $\Omega$
$D_1$ to $D_4$	$V_F = 1 \text{ V}/r_D = 10 \text{ m}\Omega$
$r_{S1} = r_{S2}$	$r_{S1} = r_{S2}$

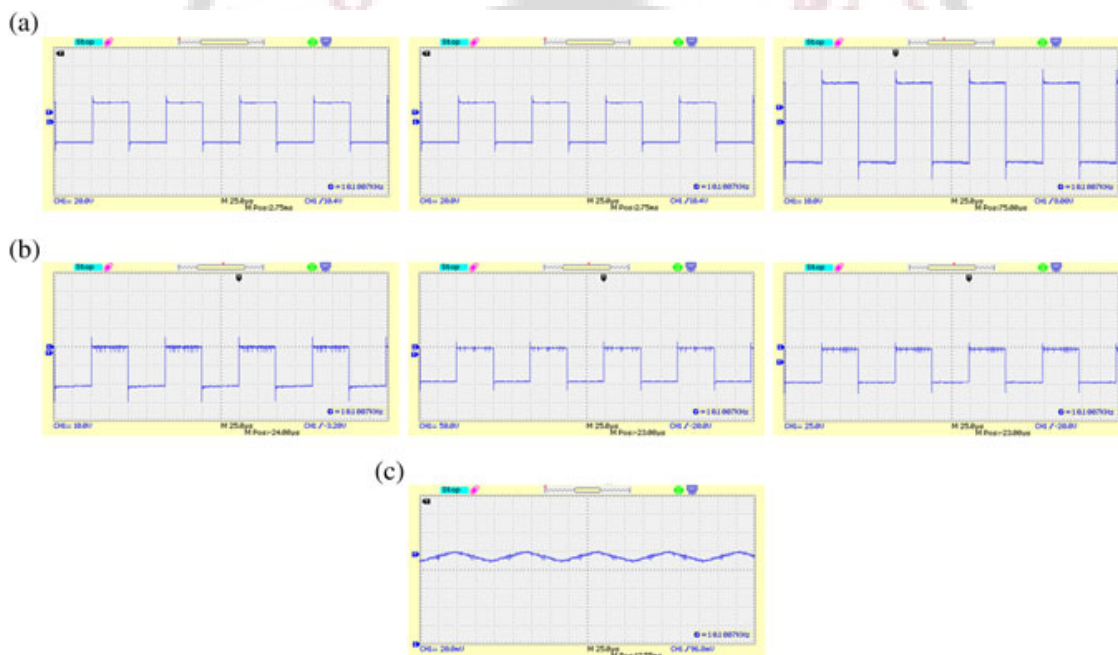


Figure 5: Simulation Results of the Proposed Multiphase DC-DC Converter

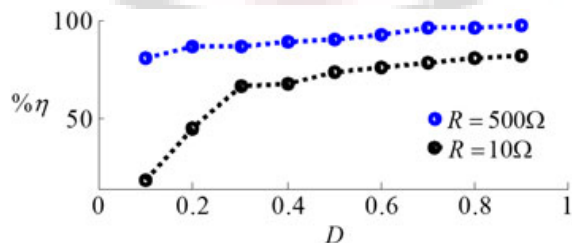


Figure 6: Comparison of Proposed Converter Efficiency for Full Load and Light Load

converter efficiency rises by increasing the load and input voltage. The maximum efficiency of proposed converter was measured nearly to 95.7% when  $V_i = 24 \text{ V}$  and  $R = 500 \Omega$ .

The dynamic response of proposed converter is analyzed with simulation results in continuous conduction mode (CCM)

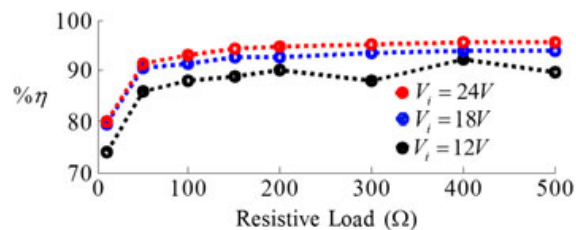


Figure 7: Comparison of Converter Efficiency Changes with the Load and Input Voltage Variations

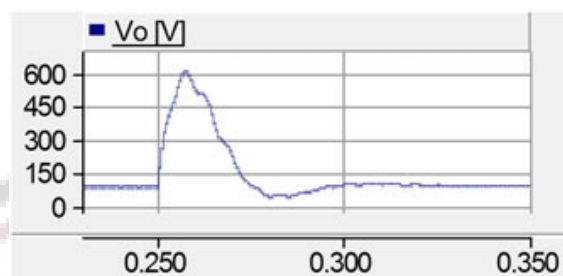


Figure 8: Dynamic Response of Proposed Converter

and considering Table 1. It is assumed that the load was increased to 100 Ω from 10 Ω at  $t = 0.25$  s. The result of this analysis was shown in Figure 8. As it is obvious, the voltage of load was reached to steady state as well when the load varied.

## V Conclusion

This paper presents a voltage-lift technique for multiphase DC-DC converter that uses voltage-lift technique, adjusts the turns ratio of the coupled inductor and achieve high step-up voltage gain. The proposed converter is highly efficient because it recycles the energy stored in the leakage inductor of the coupled inductor. Moreover, the voltage across the switch is clamped at the lower voltage level, enabling the converter to use the low rating switch to improve efficiency. This paper also describes the operating principle and the steady-state analysis in detail. Finally, a prototype converter is implemented to verify the performance of the proposed converter. In the circuit design, an simulation approach is presented to determine the duty ratio and turns ratio for high efficiency of the proposed converter. The measured results verify that this approach can assist to determine the duty ratio to achieve better efficiency performance. Additionally, the measured waveforms agree with the steady-state analysis of the continuous conduction mode (CCM) and discontinuous conduction mode (DCM) operation, and the voltage stress of switch is effectively clamped. Also, a current spike suppressing circuit is proposed to alleviate the current raising rate for the proposed converter. The simulation results verify that the proposed current spike suppressing circuit can not only reduce the current spike effectively, but also improve the conversion efficiency for the proposed converter.

## References

- [1] D. J. Dailey, *Power Supplies*. New York, NY: Springer New York, 2011, pp. 1–23. doi: [https://doi.org/10.1007/978-1-4419-9536-0\\_1](https://doi.org/10.1007/978-1-4419-9536-0_1)
- [2] R. Gastaldi and G. Campardo, *Power Supplies*. Cham: Springer International Publishing, 2020, pp. 19–44. doi: [https://doi.org/10.1007/978-3-030-45179-0\\_2](https://doi.org/10.1007/978-3-030-45179-0_2)
- [3] S. J. G. Gift and B. Maundy, *Power Supplies*. Cham: Springer International Publishing, 2021, pp. 373–409. doi: [https://doi.org/10.1007/978-3-030-46989-4\\_10](https://doi.org/10.1007/978-3-030-46989-4_10)
- [4] D. J. Dailey, *Power Supplies*. New York, NY: Springer New York, 2013, pp. 1–24. doi: [https://doi.org/10.1007/978-1-4614-4087-1\\_1](https://doi.org/10.1007/978-1-4614-4087-1_1)

- [5] U. Tietze, C. Schenk, and E. Gamm, *Power Supplies*. Berlin, Heidelberg: Springer Berlin Heidelberg, 2008, pp. 885–928. doi: [https://doi.org/10.1007/978-3-540-78655-9\\_16](https://doi.org/10.1007/978-3-540-78655-9_16)
- [6] H. Gumhalter, *Switching Mode Power Supplies*. Berlin, Heidelberg: Springer Berlin Heidelberg, 1995, pp. 176–225. doi: [https://doi.org/10.1007/978-3-642-78403-3\\_9](https://doi.org/10.1007/978-3-642-78403-3_9)
- [7] R. Kories and H. Schmidt-Walter, *Power Supplies*. Berlin, Heidelberg: Springer Berlin Heidelberg, 2003, pp. 469–512. doi: [https://doi.org/10.1007/978-3-642-55629-6\\_9](https://doi.org/10.1007/978-3-642-55629-6_9)
- [8] K. S. Rao and V. S. Chakravarthi, “Digital-controlled dual-mode switching mode power supply for low-power applications,” in *Advances in Bioinformatics, Multimedia, and Electronics Circuits and Signals*, L. C. Jain, M. Virvou, V. Piuri, and V. E. Balas, Eds. Singapore: Springer Singapore, 2020, pp. 183–195.
- [9] I. P.-Vaisband, R. Jakushokas, M. Popovich, A. V. Mezhiba, S. Köse, and E. G. Friedman, *Voltage Regulators*. Cham: Springer International Publishing, 2016, pp. 259–275. doi: [https://doi.org/10.1007/978-3-319-29395-0\\_16](https://doi.org/10.1007/978-3-319-29395-0_16)
- [10] I. Batarseh and A. Harb, *Isolated Switch-Mode DC-DC Converters*. Cham: Springer International Publishing, 2018, pp. 273–345. doi: [https://doi.org/10.1007/978-3-319-68366-9\\_5](https://doi.org/10.1007/978-3-319-68366-9_5)
- [11] B. W. Williams, *Switched-mode Power Supplies*. London: Macmillan Education UK, 1987, pp. 309–329. doi: [https://doi.org/10.1007/978-1-349-18525-2\\_15](https://doi.org/10.1007/978-1-349-18525-2_15)
- [12] I. Batarseh and A. Harb, *Soft-Switching dc-dc Converters*. Cham: Springer International Publishing, 2018, pp. 347–460. doi: [https://doi.org/10.1007/978-3-319-68366-9\\_6](https://doi.org/10.1007/978-3-319-68366-9_6)
- [13] M. Ponce-Silva, J. A. Aquí, V. H. Olivares-Peregrino, and M. A. Oliver-Salazar, “Assessment of the current-source, full-bridge inverter as power supply for ozone generators with high power factor in a single stage,” *IEEE Transactions on Power Electronics*, vol. 31, no. 12, pp. 8195–8204, Dec 2016.
- [14] G. Moschopoulos and P. Jain, “Single-phase single-stage power-factor-corrected converter topologies,” *IEEE Transactions on Industrial Electronics*, vol. 52, no. 1, pp. 23–35, Feb 2005.
- [15] T. Mishima and M. Nakaoka, “A novel high-frequency transformer-linked soft-switching half-bridge dc-dc converter with constant-frequency asymmetrical pwm scheme,” *IEEE Transactions on Industrial Electronics*, vol. 56, no. 8, pp. 2961–2969, Aug 2009.
- [16] P. Mitra, C. Dey, and R. K. Mudi, *Fuzzy PI Controller with Dynamic Set Point Weighting*. Berlin, Heidelberg: Springer Berlin Heidelberg, 2013, pp. 51–58. doi: [https://doi.org/10.1007/978-3-642-35314-7\\_7](https://doi.org/10.1007/978-3-642-35314-7_7)